Eur Biophys J (2003) 32: 578–584
DOI 10.1007/s00249-003-0305-z

BIOPHYSICS LETTER

Patrick Barré · Satoru Yamaguchi · Hazime Saitô
Daniel Huster

Backbone dynamics of bacteriorhodopsin as studied by ^{13}C solid-state NMR spectroscopy

Received: 2 January 2003 / Revised: 2 April 2003 / Accepted: 7 April 2003 / Published online: 26 June 2003

Abstract The surface dynamics of bacteriorhodopsin was examined by measurements of site-specific ^{13}C–^{1}H dipolar couplings in [3-^{13}C]Ala-labeled bacteriorhodopsin. Motions of slow or intermediate frequency (correlation time < 50 μs) scale down ^{13}C–^{1}H dipolar couplings according to the motional amplitude. The two-dimensional dipolar and chemical shift (DIPSHIFT) correlation technique was utilized to obtain the dipolar coupling strength for each resolved peak in the ^{13}C MAS solid-state NMR spectrum, providing the molecular order parameter of the respective site. In addition to the rotation of the Ala methyl group, which scales the dipolar coupling to 1/3 of the rigid limit value, fluctuations of the Cα–Cβ vector result in additional motional averaging. Typical order parameters measured for mobile sites in bacteriorhodopsin are between 0.25 and 0.29. These can be assigned to Ala103 of the C–D loop and Ala235 at the C-terminal α-helix protruded from the membrane surface, and Ala196 of the F–G loop, as well as to Ala228 and Ala233 of the C-terminal α-helix and Ala51 from the transmembrane α-helix. Such order parameters departing significantly from the value of 0.33 for rotating methyl groups are obviously direct evidence for the presence of fluctuation motions of the Ala Cα–Cβ vectors of intact preparations of fully hydrated, wild-type bacteriorhodopsin at ambient temperature. The order parameter for Ala160 from the expectantly more flexible E–F loop, however, is unavailable under highest-field NMR conditions, probably because increased chemical shift anisotropy together with intrinsic fluctuation motions result in an unresolved ^{13}C NMR signal.

Keywords ^{13}C MAS NMR · Dipolar coupling · DIPSHIFT · Membrane protein · Order parameter

D. Huster (✉)
Junior Research Group "Solid-state NMR Studies of the Structure of Membrane-associated Proteins", Biotechnological-Biomedical Center, University of Leipzig, Liebigstrasse 27, 04103 Leipzig, Germany
E-mail: husd@medizin.uni-leipzig.de
Fax: +49-341-9715709

P. Barré
Institute of Medical Physics and Biophysics, University of Leipzig, Liebigstrasse 27, 04103 Leipzig, Germany

S. Yamaguchi · H. Saitô (✉)
Department of Life Science, Himeji Institute of Technology, Harima Science Garden City, Kamigori, 678-1297 Hyogo, Japan
E-mail: saito@sci.himeji-tech.ac.jp
Fax: +81-7915-80182

Introduction

Membrane proteins, which constitute one third of the information of an expressed genome, play crucial roles in maintaining various cell functions such as transport of appropriate molecules into or out of the cell, catalysis of chemical reactions, receiving and transducing chemical signals from the cell environment and maintaining the cell structure (Branden and Tooze 1998). Membrane-associated proteins not only possess a large structural variety, they are also subject to versatile molecular dynamics in spite of the data available from 2D and 3D crystals. For instance, it appears that membrane-bound proteins like the colicin channel domain or the membrane-embedded portion of polytopic membrane proteins are intrinsically flexible (Lindeberg et al. 2000; Huster et al. 2001; Hamasaki et al. 2002). Another typical membrane protein is bacteriorhodopsin (bR) in the purple membrane of *Halobacterium salinarum*, consisting of seven transmembrane α-helices. bR is active as a proton pump and an excellent model for a variety of G-protein coupled receptors (Dencher et al. 2000; Neutze et al. 2002). It turned out that the 3D structures of the transmembrane α-helices of bR are very similar, but those of the N- or C-termini and interhelical loops are either missing or very different among the available structures from cryo-electron microscopy or

X-ray diffraction at low temperature, indicative of the presence of molecular motions (Grigorieff et al. 1996; Pebay-Peyroula et al. 1997; Essen et al. 1998; Luecke et al. 1998). In this aspect, fluorescence (Renthal et al. 1983; Marque et al. 1986), spin-labeling (Steinhoff et al. 1994) and heavy atom-labeling techniques (Krebs et al. 1993; Alexiev et al. 1998) have been utilized to examine the surface structure at ambient temperature, although these techniques are not always free of perturbations due to steric hindrance by the probes.

Solid-state NMR is an ideal tool to study the complex dynamics of membrane proteins in their natural environment, covering the entire time window of membrane protein dynamics (for reviews see Keniry et al. 1984; Opella 1986; Bowers and Oldfield 1988; Palmer et al. 1996; Siminovitch 1998; Saitô et al. 2000, 2002c). Recent site-directed ^{13}C NMR studies of [3-^{13}C]Ala-, [1-^{13}C]Ala- or Val-labeled bR revealed that the protein is heterogeneous, undergoing a variety of motions with correlation times from 10^{-2} to 10^{-8} s, depending upon the particular position of the label in the protein structure (Dencher et al. 2000; Saitô et al. 2000, 2002c). Obviously, this approach has been possible by the improved ^{13}C NMR spectral resolution available from fully hydrated bR preparations at ambient temperature that resolve 12 out of the 29 Ala and 9 out of the 21 Val residues, respectively (Tuzi et al. 2001; Yamaguchi et al. 2001; Saitô et al. 2002a, 2002b; Yonebayashi et al. 2003). Further, peak assignment has been performed by inspection of the reduced peak intensity of site-directed mutants as compared with the intensity of wild type, in addition to regiospecific assignment of peaks based on the conformation-dependent displacement of ^{13}C chemical shifts to distinguish between loop, α_I and α_{II} structures (Saitô 1986; Saitô and Ando 1989).

In this study, the amplitude of motions of the Ala residues in bR is investigated by measuring motionally averaged $^{13}C\beta$–^{1}H dipolar couplings in a site-specific manner by applying 2D solid-state NMR, correlating anisotropic dipolar couplings with isotropic chemical shift information. The ratio of motionally averaged and rigid limit dipolar coupling strength defines a molecular order parameter that decreases for increasing amplitudes of motions with a correlation time < 50 μs. Good correlation between order parameters and the respective mobile and rigid sites was found, corroborating the model of bR being a membrane protein with very heterogeneous dynamics.

Materials and methods

bR expression

[3-^{13}C]-L-Ala was purchased from Cambridge Isotope Laboratories (Andover, Mass., USA) and used without purification. *Halobacterium salinarum* S-9 was grown in TS medium in which unlabeled L-Ala was replaced by [3-^{13}C]Ala to yield [3-^{13}C]Ala-labeled bR. The purple membranes containing bR were isolated by the method of Oesterhelt and Stoeckenius (1974) and suspended in 5 mM HEPES buffer containing 0.02% NaN_3 and 10 mM NaCl at pH 7.0. Purple membranes were spun down at 40,000×*g* for 1 h. The supernatant was removed and the pellet was centrifuged again under the same conditions to further remove excess water. The sample was transferred to a 4-mm MAS rotor with a spherical insert, accommodating a sample volume of approximately 12 μL.

Solid-state NMR spectroscopy

Unless stated otherwise, all NMR experiments were carried out on a AVANCE 750 spectrometer (Bruker BioSpin, Rheinstetten, Germany), operating at a resonance frequency of 749.98 MHz for ^{1}H and 188.58 MHz for ^{13}C. A triple-resonance magic angle spinning (MAS) probe equipped with a 4 mm spinning module was used. The signal acquisition time was 50 ms. Heteronuclear two-pulse phase modulation (TPPM) decoupling with a ^{1}H radio-frequency field strength of about 40 kHz was applied during acquisition (Bennett et al. 1995). Proton and carbon 90° pulse lengths were 4.0 μs and 5.0 μs, respectively. The cross-polarization (CP) contact time and the recycle delay were 1.0 ms and 3 s, respectively. All experiments were performed at ambient temperature (20 ± 0.1 °C), with a MAS spinning rate $\omega_r/2\pi = 2500$ Hz. A sine-squared window function was applied prior to Fourier transform.

2D dipolar and chemical shift (DIPSHIFT) correlation experiments were performed using the well-known pulse sequence shown in Fig. 1A (Kolbert et al. 1990). During t_1, the ^{13}C–^{1}H dipolar interaction evolves, which requires homonuclear decoupling of the protons. ^{1}H–^{1}H homonuclear decoupling was achieved using the frequency-switched Lee–Goldburg (FSLG) sequence (Bielecki et al. 1989). The 360° proton decoupling pulses had a duration of 15.2 μs, translating into an r.f. field strength of 80 kHz along the effective field. Since the dipolar dephased signal decay is periodic with the rotor period, it was only necessary to acquire the signal

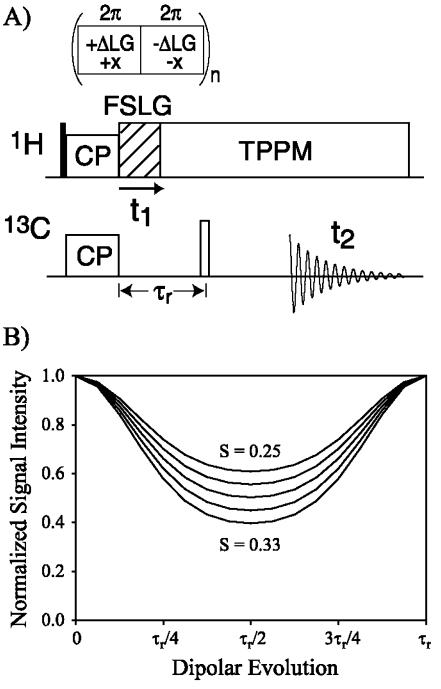

Fig. 1 **A** Pulse sequence of the constant time DIPSHIFT experiment (Kolbert et al. 1990; Hong et al. 1997). *Filled and open rectangles* refer to 90° and 180° r.f. pulses, respectively. *CP*: cross polarization, *TPPM*: heteronuclear two-pulse phase modulation decoupling. **B** Numerical simulation of the MAS time signal at a rotational frequency of 2.5 kHz for rotating CH_3 groups with order parameters of 0.25 up to 0.33 in increments of 0.02

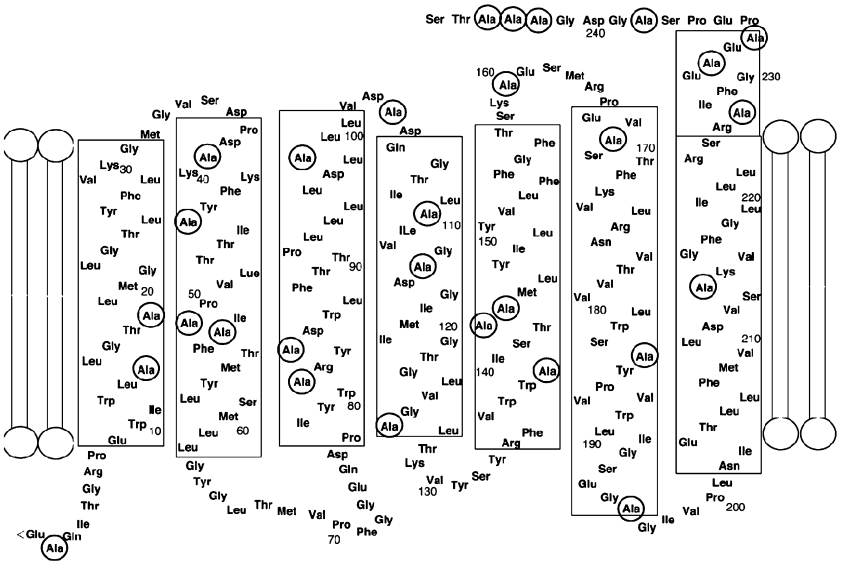

Fig. 2 Schematic representation of the 3D structure of bR with the Ala residues investigated in this study *highlighted*

over one full rotor period in the indirect dimension [constant time DIPSHIFT (Hong et al. 1997)]. A total of nine t_1 points were accumulated in the indirect dimension spaced by 1/8 of the rotor period. A numerical simulation for MAS dephasing signals of a rotating CH_3 group is given in Fig. 1B, indicating the good sensitivity of the experiment to sense small differences in dipolar couplings and molecular order parameters.

The time domain data acquired over one rotor period were fitted to numerical simulations of the dipolar dephased signal at varying coupling strength, yielding the coupling strength of interest. To obtain the true dipolar coupling value, the FSLG scaling factor of 0.577 had to be taken into account.

Simulations

The time evolution under the C–H dipolar couplings was simulated for one rotor period using a program written in Mathcad (Mathsoft, Cambridge, Mass., USA). Simulations were performed for varying C–H dipolar coupling strengths. Powder averaging was performed in 2° and 3° increments for the β and γ Euler angles, respectively. Other input parameters included the number of t_1 increments, the dwell time and the spinning rate. The simulated curves were multiplied with an exponential decay to account for T_2 relaxation effects during the dipolar evolution (the T_2 value used in these simulations was on the order of 1 ms for all sites). Best agreement between simulation and experiment was determined by the smallest r.m.s.d. values.

Results and discussion

The purpose of this study was to probe the fast dynamics of the loops and helices that are part of the bR structure. In the sample investigated, all Ala residues were ^{13}C labeled at the carbon-3 position. In Fig. 2, a schematic representation of the bR structure is given with the Ala residues highlighted.

Figure 3 illustrates the ^{13}C 1D CP-MAS spectrum of [3-^{13}C]Ala-labeled bR at a temperature of 20 °C in which 10 Ala Cβ signals were resolved, in contrast to the 12 resolved signals in the previous observation at a proton resonance frequency of 400 MHz (Yamaguchi et al. 2001; Saitô et al. 2002a, 2002b; Yonebayashi et al. 2003). In particular, the loop region (> 17 ppm) is not as well resolved at high field. Especially, the Ala160 signal from the E–F loop at 17.4 ppm is obviously missing at this high-field condition, as seen from comparison with

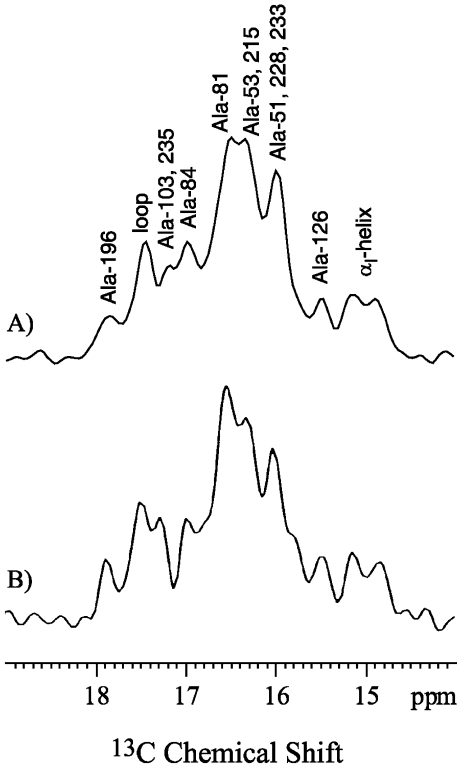

Fig. 3A 188.6 MHz ^{13}C CP MAS spectrum of [3-^{13}C]Ala bR at a spinning speed of 2.5 kHz and a temperature of 20 °C. Spectra were acquired with an acquisition time of 50 ms and TPPM decoupling with an r.f. field strength of 40 kHz. A total of 9216 transients were co-added for this spectrum. **B** ^{13}C CPMAS spectrum of the same sample at a resonance frequency of 100.64 MHz

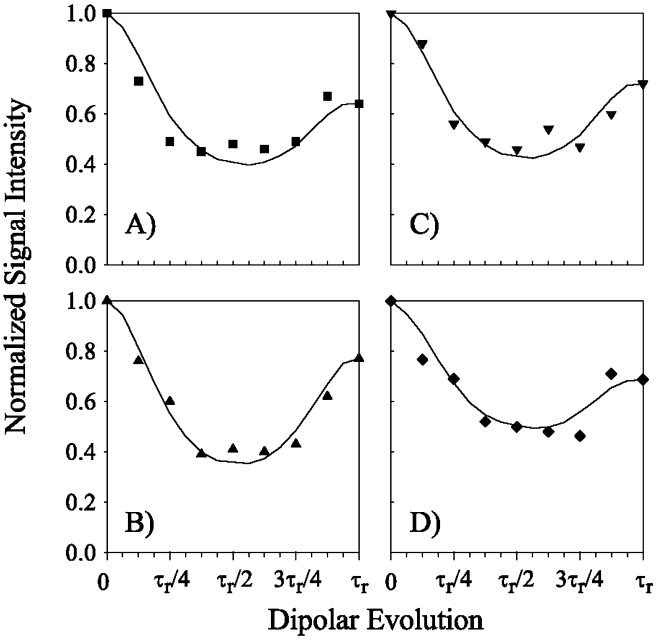

Fig. 4 ^{13}C–^{1}H dipolar dephasing curves for the signals at 16.0 ppm (**A**: Ala51, Ala228, Ala233), 16.5 ppm (**B**: Ala81), 17.0 ppm (**C**: Ala84), and 17.2 ppm (**D**: Ala103, Ala235). DIPSHIFT spectra were acquired at a spinning speed of 2.5 kHz and a temperature of 20 °C. Homonuclear FSLG decoupling with an r.f. field strength of 80 kHz was applied over one full rotor cycle. The *solid lines* represent best-fit numerical simulations with a dipolar coupling of 3.8 kHz (**A**), 4.3 kHz (**B**), 3.8 kHz (**C**) and 3.3 kHz (**D**), translating into order parameters of 0.29, 0.33, 0.29 and 0.25, respectively

the bR spectrum at 400 MHz (^{1}H Larmor frequency) (Fig. 3B). In this connection, it should be taken into account that broadening effects due to shortened T_2 relaxation times under the CP-MAS condition could be caused both by motional modulation due to internal fluctuations of dipolar interaction as well as chemical shift anisotropy, at least at higher magnetic field for the latter (Suwelack et al. 1980; Rothwell and Waugh 1981). In fact, it has been demonstrated that the longer E–F loop is most flexible, as viewed from missing density of an X-ray diffraction study on heavy atom-labeled bR (Alexiev et al. 1998).

2D DIPSHIFT experiments allow us to retrieve the dipolar coupling in the respective ^{1}H–^{13}C bond for each isotropic signal. Typical dipolar dephasing curves are shown in Fig. 4, with the best fit simulations. The dephasing curves were extracted from 2D DIPSHIFT experiments that were Fourier transformed in the direct dimension only. After a dipolar evolution time of $\tau_r/2$, the signal intensities were significantly reduced by the dipolar interaction between ^{13}C and ^{1}H in the methyl side-chains of the Ala residues. From the numerical simulation, the strength of the dipolar coupling could be extracted, scaled by the scaling factor of the homonuclear FSLG decoupling sequence. The ratio between the measured (motionally averaged) dipolar coupling and the rigid limit value (22.8 kHz) defines the order parameter, which contains information about the amplitude of the respective motion (see also Fig. 1B).

Measured dipolar couplings and their corresponding order parameters are listed in Table 1. For methyl groups undergoing free C_3 rotation around the Cα–Cβ bond, the ^{13}C–^{1}H dipolar coupling is partially averaged to result in an order parameter equal to 0.33 (Beshah et al. 1987). Further, any fluctuations of Ala Cα–Cβ vectors from residues located either at the interhelical loops or the C-terminal α-helix protruded from the membrane surface could result in an additional reduction of the molecular order parameter to become <0.33. In fact, we have previously observed that Ala residues in such locations acquire fluctuation motions with correlation times on the order of 10^{-4} and 10^{-6} s, respectively, as estimated from the suppressed peak intensities due to interference of motional frequencies with either the proton decoupling frequency or the MAS frequency, resulting in failure of the attempted peak-narrowing process for the observation of the high-resolution solid-state NMR signals (Saitô et al. 2000, 2002c). This kind of site-specific suppression of peaks was evident for bacterio-opsin in which retinal was removed from bR (Yamaguchi et al. 2000) and for a variety of mutants such as D85N at pH 10

Table 1 Assignments, dipolar couplings and order parameters of the Ala Cβ methyl signals of bR in purple membranes at a temperature of 20 °C

Signal (ppm)	Assignment[a]	Location[a]	Dipolar coupling (kHz)[b]	Order parameter[c]
14.9	–	α_I helix	4.0 ± 0.2	0.30 ± 0.02
15.2	–	α_I helix	4.3 ± 0.2	0.33 ± 0.02
15.5	Ala126 and others	Helix D, $\alpha_I$helix	4.2 ± 0.1	0.32 ± 0.01
16.0	Ala51	Helix B, α_{II}helix	3.8 ± 0.1	0.29 ± 0.01
	Ala228, Ala233	Helix G′	3.8 ± 0.1	0.29 ± 0.01
16.3	Ala53, Ala215	Helix B, Helix G, α_{II}helix	4.6 ± 0.3	0.35 ± 0.02
16.5	Ala81	Helix C	4.3 ± 0.1	0.33 ± 0.01
17.0	Ala84	Helix C	3.8 ± 0.1	0.29 ± 0.01
17.2	Ala103, Ala235	C–D loop, Helix G′	3.3 ± 0.2	0.25 ± 0.02
17.5	–	Loop	3.9 ± 0.2	0.30 ± 0.02
17.8	Ala196	F–G loop	3.6 ± 0.4	0.27 ± 0.04

[a]Assignment and location were taken from Saitô et al. (2000)
[b]Dipolar coupling as measured in a ^{13}C DIPSHIFT experiment with FSLG homonuclear decoupling (scaling factor 0.577)
[c]The full dipolar coupling in a ^{13}C–^{1}H bond is 22.8 kHz

which mimics the M-like state (Kawase et al. 2000), etc. In contrast to these observations, it is emphasized that these changes in the order parameter could be alternative evidence to indicate the presence of such fluctuation motions in the membrane proteins. Unfortunately, it is very difficult to probe such motions when Ala Cβ peaks are largely suppressed due to the presence of motional fluctuation in the order of 10^{-5} s.

Table 1 shows that the order parameters from the methyl signals at 15.5, 16.3 and 16.5 ppm, ascribable to the transmembrane α-helices, are 0.33. This finding indicates that there are no further fluctuations of the Cα–Cβ bond except for the C_3 rotation, consistent with the estimated correlation times on the order of 10^{-2} s for the majority of the transmembrane α-helices (Yamaguchi et al. 2000). These slow motions do not average the ^{1}H–^{13}C dipolar couplings; therefore, the order parameters are 0.33. Nevertheless, some signals from such transmembrane α-helices resonating at 16.0 (Ala51, Ala228 and Ala233) and 17.0 ppm (Ala84) (order parameter 0.29 ± 0.01) exhibit a somewhat reduced order parameter because they represent dynamically distorted α_{II} helices with low-frequency anisotropic motions (Kimura et al. 2002).

In contrast, it is expected that Ala residues in the loops are subject to such fluctuation motions with shorter correlation times, as also demonstrated from the suppressed ^{13}C NMR peaks from [1-^{13}C]Ala-labeled bR, due to interference of motional frequency with the frequency of MAS (Saitô et al. 2002b). This turned out to be the case, because the most reduced order parameter of 0.25 is observed for the peak at 17.2 ppm, ascribed to Ala103 in the C–D loop and Ala235 from the C-terminal α-helix, consistent with a view of the largest motional amplitude. Further, the order parameter of Ala196 resonating at 17.8 ppm is shown as 0.27 ± 0.02, because this residue is located at the rather flexible F–G loop. Unfortunately, the order parameter at Ala160 from the E–F loop is unavailable from the unresolved peak mentioned above under this high-field condition, although the most reduced order parameter of less than 0.25 should be expected from this Ala160 located at the longer E–F loop among the loops in bR. These findings indicated that the Ala residues located at the C–D, E–F and F–G loops are really not static, at least at ambient temperature, but undergoing flexible motions with a time scale on the order of 10^{-5} s. This is obviously in contrast to a static picture of turned structures as found for a number of crystalline globular proteins (Branden and Tooze 1998) at low temperature. Unfortunately, there are no data for the A–B and B–C loops because of lack of Ala residues in these structures (see Fig. 2).

As pointed out already, the two Ala residues Ala228 and Ala233, located in the C-terminal α-helix (helix G′), are superimposed with the Ala51 from the helix B at 16.0 ppm. The estimated correlation times for these residues are on the order of 10^{-6} s, as inferred from the measured spin–spin relaxation times under proton irradiation (Yamaguchi et al. 2001; Saitô et al. 2002a). In this case, it is well recognized that their order parameter might be reduced from the value of rather static α-helix located within the bilayer. This is also consistent with our previous finding about the prolonged carbon-resolved proton $T_{1\rho}$ value of 11.2 ms for the peak at the C-terminal α-helix in bacterio-opsin as compared with those of others in the order of 6 ms (Tuzi et al. 1996). Thus, the reduced order parameter for 0.29 ± 0.01 is caused by fluctuation motions of low or intermediate frequency (10^{4}–10^{5} Hz), although the superposed Ala51 peak from the transmembrane α-helix may have an opposite effect to such a reduced order parameter.

Our results are in good agreement with the *B* factors of X-ray investigations (Luecke et al. 1998) and molecular dynamics simulations (Woolf 1997). Most clearly, this can be demonstrated for Ala81 and Ala84 that both reside in helix C, having high order parameters and correspondingly low *B* factors of 11.24 and 6.79, respectively (see Fig. 5a). In contrast, Ala196 in the F–G loop has a lower order parameter and a much higher *B* factor of 33.21 (Fig. 5B). Also, molecular dynamics simulations indicate that the mobility in bR is unequally distributed between the different helices; however, the time window is rather short and many types of motions are not sampled in these simulations (Woolf 1997). For the Ala residues in helices B, D and G, small r.m.s. deviations of the Cα site on the order of 2–3 Å have been found, in agreement with the high order parameters we have found in our solid-state NMR study. In the simulation, helix D is more dynamically disordered with r.m.s. deviations of Ala126 on the order of 4 Å, which is in slight contrast to the high order parameter of 0.32

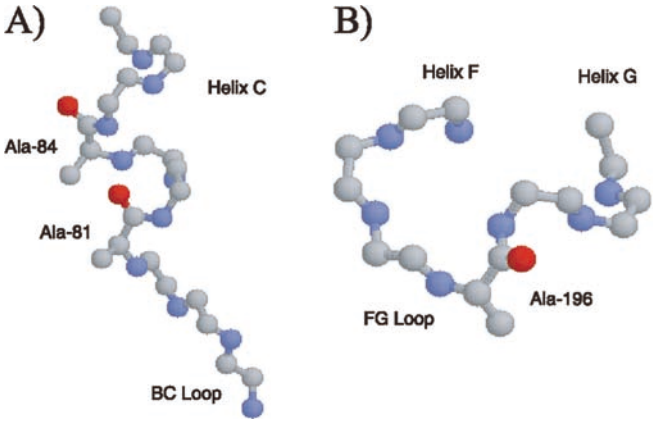

Fig. 5 Schematic representation of the helix C–BC loop region (residues Ile78 to Leu87, **A**) and the F–G loop region of bR (residues Ser193 to Val199, **B**) according to the crystal structure by Luecke et al. (1998). Ala81 and Ala84 both reside in the rigid helix C with order parameters of 0.29 and 0.33, respectively. The crystal structure shows *B* factors of 11.24 (Ala81) and 6.79 (Ala84) for these rigid Ala sites. Larger amplitude motions with an order parameter of 0.27 have been found for Ala196 (**B**); accordingly, higher *B* factors of 33.21 have been obtained in the crystal structure. All sidechains except for Ala have been omitted for clarity; carbon atoms are shown in *gray*, nitrogen in *blue* and oxygen in *red*

found in our study. Unfortunately, the loop regions were not included in the molecular dynamics simulation.

In conclusion, it is demonstrated that the observation of the reduced order parameters in the ^{13}C NMR spectrum of [3-^{13}C]Ala-labeled bR can be utilized as an alternative means to examine internal fluctuation motions on the millisecond or microsecond timescale relevant to a variety of biological functions. This approach is, of course, not applicable to the situation in which motional frequency is very close to either frequency of proton decoupling or magic angle frequency, to result in complete suppression of peaks.

Acknowledgements The junior research group is funded by the Saxon State Ministry of Higher Education, Research and Culture. The work was supported by the Deutsche Forschungsgemeinschaft (Ar-195/8-1). This work was also supported in part by a grant-in-aid for Scientific Research from KAKENHI from MEXT of Japan.

References

Alexiev BW, Mollaaghaba RG, Khorana HG, Heyn MP (1998) Structure of the interhelical loops and carboxyl terminus of bacteriorhodopsin X-ray diffraction using site-directed-atom labeling. Biochemistry 37:10411–100419

Bennett AE, Rienstra CM, Auger M, Lakshmi KV, Griffin RG (1995) Heteronuclear decoupling in rotating solids. J Chem Phys 103:6951–6958

Beshah K, Olejniczak ET, Griffin RG (1987) Deuterium NMR study of methyl group dynamics in L-alanine. J Chem Phys 86:4730–4736

Bielecki A, Kolbert AC, Levitt MH (1989) Frequency-switched pulse sequences: homonuclear decoupling and dilute spin NMR in solids. Chem Phys Lett 155:341–345

Bowers JL, Oldfield E (1988) Quantitative carbon-13 nuclear magnetic resonance spectroscopy study of mobile residues in bacteriorhodopsin. Biochemistry 27:5156–5161

Branden C, Tooze J (1998) Introduction to protein structure. Garland, New York

Dencher NA, Sass HJ, Buldt G (2000) Water and bacteriorhodopsin: structure, dynamics, and function. Biochim Biophys Acta 1460:192–203

Essen L, Siegret R, Lehmann WD, Oesterhelt D (1998) Lipid patches in membrane protein oligomers: crystal structure of the bacteriorhodopsin-lipid complex. Proc Natl Acad Sci USA 95:11673–11678

Grigorieff N, Ceska TA, Downing KH, Baldwin JM, Henderson R (1996) Electron-crystallographic refinement of the structure of bacteriorhodopsin. J Mol Biol 259:393–421

Hamasaki N, Abe Y, Tanner MJ (2002) Flexible regions within the membrane-embedded portions of polytopic membrane proteins. Biochemistry 41:3852–3854

Hong M, Gross JD, Griffin RG (1997) Site-resolved determination of peptide torsion angle Φ from relative orientations of backbone N-H and C-H bonds by solid-state NMR. J Phys Chem 101:5869–5874

Huster D, Xiao L, Hong M (2001) Solid-state NMR investigation of the dynamics of soluble and membrane-bound colicin Ia channel-forming domain. Biochemistry 40:7662–7674

Kawase Y, Tanio M, Kira A, Yamaguchi S, Tuzi S, Naito A, Kataoka M, Lanyi JK, Needleman R, Saitô H (2000) Alteration of conformation and dynamics of bacteriorhodopsin induced by protonation of Asp 85 and deprotonation of Schiff base as studied by ^{13}C NMR. Biochemistry 39:14472–14480

Keniry MA, Gutowsky HS, Oldfield E (1984) Surface dynamics of the integral membrane protein bacteriorhodopsin. Nature 307:383–386

Kimura S, Naito A, Tuzi S, Saitô H (2002) Dynamics and orientation of transmembrane peptide from bacteriorhodopsin incorporated into lipid bilayer as revealed by solid state ^{31}P and ^{13}C NMR spectroscopy. Biopolymers 63:122–131

Kolbert AC, de Groot HJM, Levitt MH, Munowitz MG, Roberts JE, Harbison GS, Herzfeld J, Griffin RG (1990) Two-dimensional dipolar-chemical shift NMR in rotating solids. In: Granger P, Harris RK (eds) Multinuclear magnetic resonance in liquids and solids – chemical applications. Kluwer, Dordrecht, pp 339–54

Krebs MP, Behrens W, Mollaaghababa RG, Khorana HG, Heyn MP (1993) X-ray diffraction of a cystein-containing bacteriorhodopsin mutant and its mercury derivative. Localization of an amino acid residue in the loop of an integral membrane protein. Biochemistry 32:12830–12834

Lindeberg M, Zakharov SD, Cramer WA (2000) Unfolding pathway of the colicin E1 channel protein on a membrane surface. J Mol Biol 295:679–692

Luecke H, Richter HT, Lanyi JK (1998) Proton transfer pathways in bacteriorhodopsin at 2.3 angstrom resolution. Science 280:1934–1937

Marque J, Kinoshita K Jr, Govindjee R, Ikegami A, Ebrey TG, Otomo J (1986) Environmental modulation of C-terminal dynamic structure in bacteriorhodopsin. Biochemistry 25:5555–5559

Neutze R, Pebay-Peyroula E, Edman K, Royant A, Navarro J, Landau EM (2002) Bacteriorhodopsin: a high-resolution structural view of vectorial proton transport. Biochim Biophys Acta 1565:144–167

Oesterhelt D, Stoeckenius W (1974) Isolation of the cell membrane of *Halobacterium halobium* and its fractionation into red and purple membrane. Methods Enzymol 31:667–678

Opella SJ (1986) Protein dynamics by solid state nuclear magnetic resonance. Methods Enzymol 131:327–361

Palmer AG III, Williams J, McDermott A (1996) Nuclear magnetic resonance studies of biopolymer dynamics. J Phys Chem 100:13293–13310

Pebay-Peyroula E, Rummel G, Rosenbusch JP, Landau EM (1997) X-ray structure of bacteriorhodopsin at 2.5 angstroms from microcrystals grown in lipidic cubic phases. Science 277:1676–1681

Renthal R, Dawson N, Tuley J, Horowitz P (1983) Constraints on the flexibility of bacteriorhodopsin's carboxyl terminal tail at the purple membrane surface. Biochemistry 22:5–11

Rothwell WP, Waugh JS (1981) Transverse relaxation of dipolar coupled spin systems under rf irradiation: detecting motions in solids. J Chem Phys 74:2721–2732

Saitô H (1986) Conformation-dependent ^{13} C chemical shifts: a new means of conformational characterization as obtained by high-resolution solid-state ^{13}C NMR. Magn Reson Chem 24:835–852

Saitô H, Ando I (1989) High-resolution solid-state NMR studies on synthetic and biological macromolecules. Annu Rep NMR Spectrosc 21:209–290

Saitô H, Tuzi S, Yamaguchi S, Tanio M, Naito A (2000) Conformation and backbone dynamics of bacteriorhodopsin revealed by ^{13}C-NMR. Biochim Biophys Acta 1460:39–48

Saitô H, Kawaminami R, Tanio M, Arakawa T, Yamaguchi S, Tuzi S (2002a) Dynamic aspect of bacteriorhodopsin as viewed from C-13 NMR: conformational elucidation, surface dynamics and information transfer from the surface to inner residues. Spectrosc Int J 16:107–120

Saitô H, Tsuchida T, Ogawa K, Arakawa T, Yamaguchi S, Tuzi S (2002b) Residue-specific millisecond to microsecond fluctuations in bacteriorhodopsin induced by disrupted or disorganized two-dimensional crystalline lattice, through modified lipid-helix and helix-helix interactions, as revealed by ^{13}C NMR. Biochim Biophys Acta 1565:97–106

Saitô H, Tuzi S, Tanio M, Naito A (2002c) Dynamic aspect of membrane proteins and membrane associated peptides as revealed by ^{13}C NMR: lessons from bacteriorhodopsin as an intact protein. Annu Rep NMR Spectrosc 47:39–108

Siminovitch DJ (1998) Solid-state NMR studies of proteins: the view from static ^{2}H NMR experiments. Biochem Cell Biol 76:411–422

Steinhoff HJ, Mollaaghababa RG, Altenbach C, Hideg K, Krebs M, Khorana HG, Hubbel WL (1994) Time-resolved detection of structural changes during the photocycle of spin-labeled bacteriorhodopsin. Science 266:105–117

Suwelack D, Rothwell WP, Waugh JS (1980) Slow molecular motion detected in the NMR spectra of rotating solids. J Chem Phys 73:2559–2569

Tuzi S, Yamaguchi S, Naito A, Needleman R, Lanyi JK, Saitô H (1996) Conformation and dynamics of [3-^{13}C]Ala-labeled bacteriorhodopsin and bacterioopsin, induced by interaction with retinal and its analogs, as studied by ^{13}C nuclear magnetic resonance. Biochemistry 35:7520–7527

Tuzi S, Hasegawa J, Kawaminami R, Naito A, Saitô H (2001) Regio-selective detection of dynamic structure of transmembrane alpha-helices as revealed from ^{13}C NMR spectra of [3-^{13}C]Ala-labeled bacteriorhodopsin in the presence of Mn^{2+} ion. Biophys J 81:425–434

Woolf TB (1997) Molecular dynamics of individual α-helices of bacteriorhodopsin in dimyristoyl phosphatidylcholine. I. Structure and dynamics. Biophys J 73:2376–2392

Yamaguchi S, Tuzi S, Tanio M, Naito A, Lanyi JK, Needleman R, Saitô H (2000) Irreversible conformational change of bacterioopsin induced by binding of retinal during its reconstitution to bacteriorhodopsin, as studied by ^{13}C NMR. J Biochem (Tokyo) 127:861–869

Yamaguchi S, Yonebayashi K, Konishi H, Tuzi S, Naito A, Lanyi JK, Needleman R, Saitô H (2001) Cytoplasmic surface structure of bacteriorhodopsin consisting of interhelical loops and C-terminal alpha helix, modified by a variety of environmental factors as studied by ^{13}C-NMR. Eur J Biochem 268:2218–2228

Yonebayashi K, Yamaguchi S, Tuzi S, Saitô H (2003) Cytoplasmic surface structures of bacteriorhodopsin modified by site-directed mutations and cation binding as revealed by ^{13}C NMR. Eur Biophys J 32:1–11